Princeton Plasma Physics Laboratory

PPPL- 4931

PPPL- 4931

Performance Evaluation of K-DEMO Cable-in-Conduit Conductors Using the Florida Electro-Mechanical Cable Model

Yuhu Zhai, et. al.

JULY, 2013

PPPL PRINCETON PLASMA PHYSICS LABORATORY

Prepared for the U.S. Department of Energy under Contract DE-AC02-09CH11466.

Princeton Plasma Physics Laboratory
Report Disclaimers

Full Legal Disclaimer

Trademark Disclaimer

PPPL Report Availability

Princeton Plasma Physics Laboratory:

http://www.pppl.gov/techreports.cfm

Office of Scientific and Technical Information (OSTI):

http://www.osti.gov/bridge

Related Links:

U.S. Department of Energy

Office of Scientific and Technical Information

Fusion Links

Performance Evaluation of K-DEMO Cable-in-Conduit Conductors using the Florida Electro-Mechanical Cable Model

Yuhu Zhai, Keeman Kim, Peter Titus and Thomas Brown

***Abstract*—The Korean DEMO Tokamak fusion power plant (K-DEMO) is currently under a preliminary conceptual design study for its engineering feasibility for steady-state operation. K-DEMO is planned to have two phases aimed at demonstrate a reasonable net-electricity (> 300 MW) generation with a minimum cost while providing a maximum flexibility. Since K-DEMO plans to use high performance Nb_3Sn strands and cable-in-conduit conductors (CICCs) for the design of its magnet coils, potential performance degradation of CICCs will be a critical issue as we have seen in ITER, which is currently under construction in the south of France. The critical current observed in most ITER CICC test samples is significantly lower than expected and the voltage-current characteristic is seen to have a much broader transition from a single strand to a CICC cable. We apply Florida Electro-Mechanical Cable Model (FEMCAM) developed in the past to evaluate the design of K-DEMO CICCs and provide performance evaluation for K-DEMO CS and TF modules. FEMCAM combines the thermal bending effect during cool down after heat treatment and the electromagnetic bending effect due to locally accumulating Lorentz force during magnet operation. It also includes effect of strand filament fracture and related local current sharing observed in SULTAN for ITER for the cable n-value calculation. The model has been benchmarked previously against over 40 different CICC tests.**

***Index Terms*—Cable-in-Conduit Conductor, high performance Nb_3Sn strand, Fusion Magnet, K-DEMO.**

I. Introduction

The Korean DEMO Tokamak fusion power plant is currently under a preliminary conceptual design study for its engineering feasibility for steady-state operation. K-DEMO is planned to have two phases aimed at demonstrate a reasonable net-electricity (> 300 MW) generation with a minimum cost while providing a maximum flexibility [1]. Fig. 1 presents a cut-away view of the core arrangement for the K-DEMO fusion reactor. A magnetic field at the plasma center higher than 8 T can be achieved by using the currently available high performance Nb_3Sn strands with J_c (12 T, 4.2 K) > 2600 A/mm^2. The advanced high J_c strands have been used in cable-in-conduit conductors (CICCs) for the European dipole (EDIPO) magnet installed next to SULTAN facility and recently tested successfully in reaching its designed full field. Performance degradation of Nb_3Sn CICCs is a critical issue as we have seen in ITER which is currently under construction in the south of France. The critical current observed in ITER CICC tests is significantly lower than expected and the voltage-current characteristic is seen to have a much broader transition from a single strand to a CICC cable.

Florida Electro-Mechanical Cable Model (FEMCAM) is used to evaluate the design of K-DEMO CICCs and provide performance evaluation for the K-DEMO CS and TF modules. FEMCAM combines the thermal bending effect during cool down due to differential thermal contraction and the electromagnetic bending effect due to locally accumulating Lorentz force during magnet operation [2]-[3]. The model has been used previously for evaluating high performance CICCs made of advanced J_c strands for the EDIPO magnet and the series-connected hybrid magnet currently under construction at the NHMFL. It also includes strand effect of filament fracture and related local current sharing observed in SULTAN for ITER for the cable n-value evaluation.

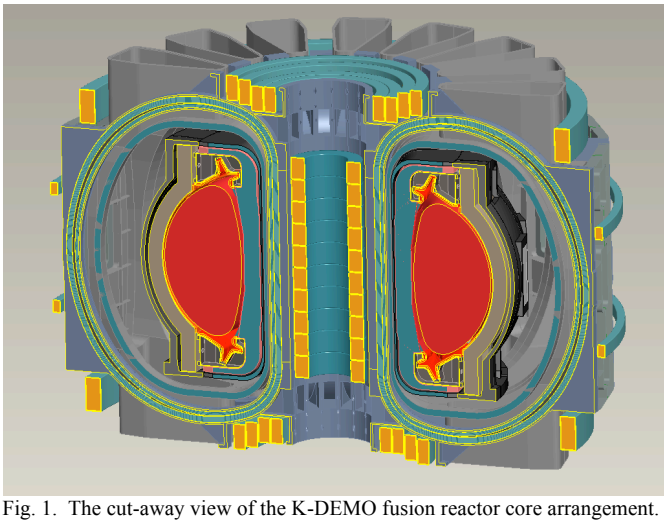

Fig. 1. The cut-away view of the K-DEMO fusion reactor core arrangement.

II. K-DEMO Conductor Parameters

A. TF CICC Parameters

K-DEMO Toroidal Field (TF) conductors are graded into two types of CICC based on the magnetic field distribution on the TF coils. The high field region TF CICC runs 65.5 kA net

Manuscript received July 16, 2013. This work was supported in part by the U.S. Department of Energy under contract number DE-AC02-09CH1 1466 (PPPL) and the Korean National Fusion Research Institute.

Y. Zhai (corresponding author), P. Titus and T. Brown are with Princeton Plasma Physics Laboratory, Princeton, NJ 08540 USA (Phone: 609-243-3056; fax: 609-243-3248; e-mails: yzhai@pppl.gov, ptitus@pppl.gov, tbrown@pppl.gov.

K. Kim is with the Advanced Project Division, National Fusion Research Institute, Daejeon, 305-806 South Korea (e-mail: kkeeman@nfri.re.kr).

current using cable of 1800 high J_c Nb_3Sn strands inside a steel jacket. The cable is cooled by forced flow helium in the 28.1% void space and a helical spiral cooling channel. Fig. 2 (left) presents the K-DEMO high field TF CICC cross-section. The peak field in the high field CICCs is ~16 T. The high field CICC has a rectangular cross section with an aspect ratio of 2.2 to reduce a transverse IB/h pressure

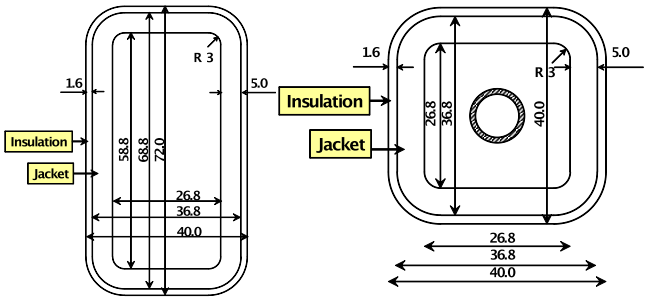

Fig. 2. Conductor cross section of K-DEMO TF CICC (left) and the small TF CICC (right) with a central cooling channel.

load transferred by the cable during magnet operation.

B. Small TF CICC Parameters

The small TF CICC has a square-shape cross section and using cable of 360 Nb_3Sn strands and 402 copper strands as shown in Fig. 2 (right). Peak field in the small field TF CICC is 12.1 T. The small TF CICC has ~27.1% void fraction and a central cooling channel.

C. CS CICC Parameters

Due to a general higher number of cyclic loading required for the CS operation and the potential concern of continuing degradation upon cyclic loading, K-DEMO CS CICCs use a less advanced OST strand similar to ITER strands with J_c ~1000 A/mm^2. The CS CICC runs 42 kA current using cable made of 576 Nb_3Sn strands and 288 copper strands twisted together. It has a rectangular-shape cross section as shown in Figure 3. The void fraction measured in CS CICC is ~32.5%.

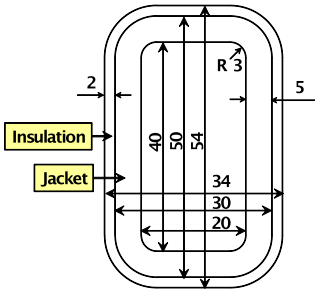

Fig. 3. The K-DEMO CS CICC conductor cross section.

D. Conductor Test Samples

Table I listed the TF and CS strand, cable, steel jacket and the CICC design parameters. The transverse pressure on the high field TF and CS CICCs is below 20 MPa (common to ITER CICCs) but close to 30 MPa on the K-DEMO small TF CICC. Fig. 4 presents photos of K-DEMO CICC samples that have been made for conductor tests.

TABLE I
TF AND CS CICC PARAMETERS

	Parameters	TF CICC	Small TF	CS CICC
Strand	diameter	0.82 mm	0.82 mm	0.82 mm
	Cu/non-Cu ratio	1	1	1
	J_c (12 T, 4.2 K)	>2600 A/mm^2	>2600 A/mm^2	~1050 A/mm^2
Cable	No. of s/c strands	1800	360	576
	No. of Cu strands	0	402	288
	void fraction	28.1%	27.23%	32.5%
	cabling pattern	3x4x5x6x5	((2sc+2cu)x5 x6+7cu)x6	3x3x4x4x6
	cable twist pitch	80x140x190x245 x385	80x140x190 x300	20x45x85x150x355
Jacket	material	SS316LN	SS316LN	SS316LN
	thickness	5 mm	5 mm	5 mm
CICC	operating current	65.5 kA	65.5 kA	42 kA
	peak field	16 T	12.1 T	12.48 T
	IB/h	17.8 MPa	29.58 MPa	13.1 MPa

No vertical lines in table.

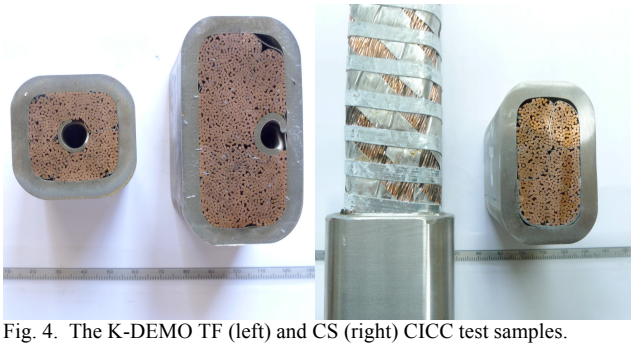

Fig. 4. The K-DEMO TF (left) and CS (right) CICC test samples.

III. FEMCAM FORMULATION

Strain sensitivity of multi-filamentary Nb_3Sn strands has been well known for decades. The idea of J_c degradation due to bending and transverse compression was first introduced by Ekin in 1980s [4]. FEMCAM previously developed for modeling CICC performance degradation for the high field magnets is based on a beam bending formulation of cabled-strand under both thermal and locally accumulated Lorentz loads [4]-[5]. In FEMCAM, cabled strands were assumed to have a 2D waviness shape simplified from the real multi-stage helix in a 3D cable. The model was benchmarked against over 40 CICC tests and has been used for the evaluation of CICCs using advanced J_c strands such as the OST dipole strands for the EDIPO magnet and the series-connected hybrid magnets at NHMFL. The EDIPO magnet was recently tested successfully in CRPP sitting next to SULTAN facility to reach its designed full field [8].

A. Thermal Bending during Cool Down

Thermal bending strain calculation of Nb_3Sn CICCs during cool down after heat treatment was first introduced in [6], based on Timoshenko beam-column theory [9]. During cool down, the steel conduit contracts much more than a strand due to the differential thermal expansion. As a result, thermal compressive forces on the strands create a large local axial compressive strain as well as a local bending strain on individual strands. Thermal bending plays an important role in

CICC performance degradation as we have seen in previous FECAM benchmark study [2].

B. Electromagnetic Bending under Lorentz Force

Bending strain due to locally accumulated magnetic load is calculated based on a multi-stage beam bending formulation initially proposed in [7]. The model formulation was described as result of strand mechanical interactions within a CICC by bending of clamped beams and pinching due to contact stress at strand crossings.

C. Strand Contact and Current Transfer

FEMCAM also includes I_c degradation due to transverse compression on strands at crossing and the effect of filament fracture for potential irreversible degradation. We assume filament critical current drops to zero in Ekin's integration [4] if filament tensile strain is greater than the strand irreversible strain limit. We assume full current transfer between strands and add all current from layer to layer to obtain the average cable critical current degradation.

D. Axial Thermal Compressive Strain

The axial thermal compressive strain on Nb_3Sn after cool down is previously believed to be ~0.65% for a stainless steel jacket CICC. Resent SULTAN experimental studies, however, showed that the cable in high field zone is strain relaxed inside the jacket and the thermal compressive strain measured is -0.35%~-0.45% for ITER tested CICCs [10].

IV. CICC Performance Evaluation

A. High Performance Nb_3Sn Strands

The advanced OST dipole strands with J_c ~2600 A/mm^2 are used for the K-DEMO TF conductor performance evaluation. The ITER-type OST strands with J_c ~1000 A/mm^2 are used for K-DEMO CS CICC evaluation. An assumed 0.15% hoops strain is included in the TF and CS evaluation. The strand scaling parameters are listed in Table II [12]-[13]. Additional input parameters include the strand axial modulus 35 GPa and a transverse modulus 3.5 GPa. The axial thermal compressive strain is assumed to be ~0.45% [10]. A bending wavelength of 7 mm and 5 mm is used for the TF and CS CICC respectively, based on the long and short twist pitch used for TF and CS cables. The strain sensitivity of OST dipole strand critical current was shown in Fig. 5 at the TF CICC nominal condition. Fig. 6 shows strain sensitivity of ITER OST strand for K-DEMO CS evaluation. Fig. 7 presents J_c degradation due to bending of the OST dipole strand with and without assumed filament fracture for both no current transfer and full current transfer cases. It clearly shows the J_c degradation due to bending of the advanced Nb_3Sn strands if filament fracture beyond the irreversible strain limit is introduced in the analysis. Impact of filament fracture is much less for Bronze strands with a higher irreversible strain limit. With rapid advance of wire fabrication technology, the situation will be greatly improved for internal tin strands in the new few years.

TABLE II
STRAND SCALING PARAMETERS FOR K-DEMO CICC EVALUATION

Scaling parameters	TF CICC OST Dipole strand	CS CICC OST ITER strand
C=	46980	16317/18707
B^*_{c20max}	29.28 T	33.79 T
T^*_{c0max}	15.94 K	16.1 K
Ca_1	59.36	44.97
Ca_2	23.91	0
e0,a	0.309%	0.284%
e_m	-0.11%	-0.09%
p	0.5	0.54
q	2	2.1
irreversible limit	0.05%	0.3%

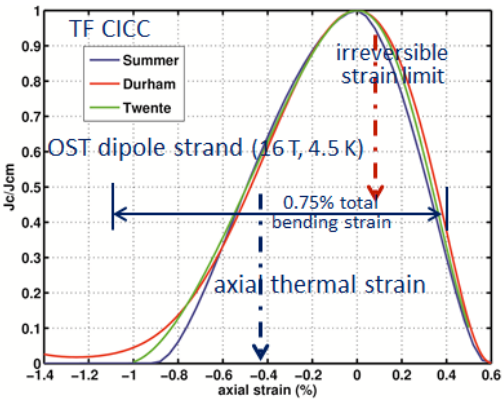

Fig. 5. Strain sensitivity of OST dipole strand for K-DEMO TF CICC evaluation. The peak total bending strain is ~0.75% for TF CICC strands.

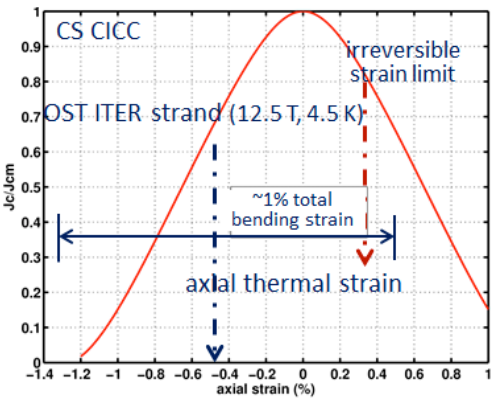

Fig. 6. The strand strain sensitivity of ITER OST strand for K-DEMO CS CICC evaluation. The peak bending strain is ~1% for CS CICC strands.

Fig. 7. OST strand bending characteristics with full filament current transfer (LRL) and no filament current transfer (HRL) for K-DEMO CICC evaluation. Blue curves show the effect of filament fracture where a conservative assumption of J_c drops to zero is used for filament bending strain beyond the irreversible limit.

B. CICC 1st Cycle Performance

Table III presents peak bending strains in K-DEMO CICCs and Table IV presents FEMCAM predicted 1st cycle CICC performance, where transverse load degradation for the case of assuming no filament fracture is compared with the case of assuming filament fracture. The large difference between the two cases is mainly due to conservative assumption made to have the J_c drop to zero for filaments with bending strain beyond the irreversible limit.

C. CICC Performance under Cyclic Loading

CICC performance upon cyclic loading is more relevant to the CS magnet operation where a significant number of EM load cycles may be expected for the lifetime of K-DEMO. The excess strain effect previously introduced in FEMCAM benchmark study for fatigue evaluation can be used here. Fig. 8 presents additional I_c degradation vs. the excess strain for CICCs using the advanced J_c strands. The blue curve line indicates a transition region between little and large addition

TABLE III
STRAND PEAK BENDING STRAIN IN K-DEMO TF AND CS CICCS

bending strain (%)	thermal	EM	total	excess strain
TF CICC	0.34	0.41	0.75	0.35
Small TF CICC	0.34	0.37	0.71	0.31
CS CICC	0.29	0.7	0.99	0.39

degradation upon cyclic loading. The K-DEMO TF CICCs with an excess strain of ~0.35% is expected to have ~5% additional degradation upon cyclic loading of TF module. The CS CICCs has a slightly higher excess strain ~0.39% due to its higher void fraction, where 5~10% additional degradation is expected.

D. Modeling of Transition broadening

Recent development of FEMCAM includes modeling of the transition broadening of CICCs upon EM cyclic loading for the extreme cases seen in SULTAN tested ITER CICCs to

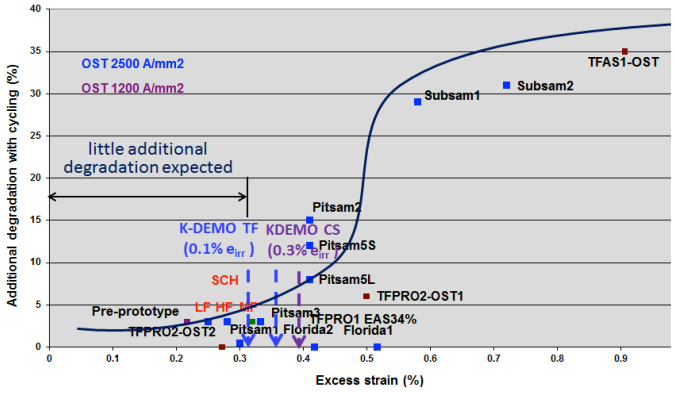

Fig. 8. Additional degradation against excess strain in CICCs

study conductor irreversible degradation [11]. Fig. 9 shows the FEMCAM modeled electric field vs. T_{cs} transition of ITER CSIO1 CICC at 1st and after 5000 EM load cycles. The model included a measured axial compressive strain increase upon cyclic loading due to high field zone potential cable local ratcheting [11].

V. CICC DESIGN IMPLICATION

FEMCAM analysis showed that K-DEMO TF and CS

TABLE IV
FEMCAM PREDICTED K-DEMO CICC 1ST CYCLE PERFORMANCE

Performance	TF CICC	Small TF CICC	CS CICC
Transverse load degradation (%) (no fracture/with fracture)	16.8/30.8	10.1/22.4	18.3/26.4
Cable n-value	9.61/10.7	17.3/19.6	11.7/12.4
Cable Tcs (K)	6.14/6.08	6.54/6.46	6.81/6.74
Excess strain (%)	0.35	0.31	0.39

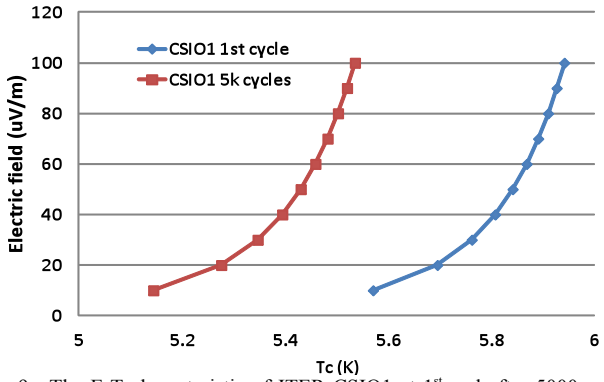

Fig. 9. The E-T characteristic of ITER CSIO1 at 1st and after 5000 cycles showed reduced current sharing temperature upon cyclic loading due to cable local ratcheting where more compressive strain is observed upon cycling. Similar situation can happen for K-DEMO CS CICC using the same strands.

CICCs may have 10-30% I_c degradation at the initial load cycle. The TF CICCs are expected to have 5% additional degradation with cyclic loading due to the greater than 0.3% excess strain. The CS CICCs, however, may have a slightly higher additional degradation due to a higher excess strain as a result of higher void fraction. The short twist pitch used for K-DEMO CS CICC is consistent with that used in the most recent ITER CS CICCs successfully tested.

VI. CONCLUSION

FEMCAM was used to evaluate conductor performance for the K-DEMO TF and CS magnets using advanced Nb_3Sn strands with bending strain sensitivity. FEMCAM predicted 10-30% I_c degradation mainly because K-DEMO high field TF CICC is in a peak field of 16 T. Higher cable void fraction in CS CICC resulted a slightly higher fatigue related excess strain. Although a very small additional I_c transverse load degradation upon EM load cycling is expected for K-DEMO CICCs, local cable softening due to ratcheting similar to some ITER CS CICC tests may happen. FEMCAM predicted over 1.5 K temperature margin for the TF and CS conductors respectively. As K-DEMO is expected to be operating predominately at 90% of its peak field level, the field reduction may boost temperature margin ~0.5-0.7 K for the TF CICCs and ~1 K for the CS CICCs.

ACKNOWLEDGMENT

This research was partially supported by the Korean

National Fusion Research Institute under a research agreement with Princeton University.

REFERENCES

[1] K. Kim, S. Oh, S.H. Baek, P. Titus, T. Brown, C. Kessel and Y. Zhai, "A preliminary conceptual design study for Korean fusion DEMO reactor magnets*," 25th Symposium on Fusion Engineering*, Submitted for publication, Jun. 2013.

[2] Y. Zhai, and Mark Bird, "Florida electro-mechanical cable model of Nb_3Sn CICCs for high field magnet design", *Supercond. Sci. Technol*., vol.21, 115010, 2008.

[3] Y. Zhai, "Electro-mechanical modeling of Nb_3Sn CICC performance degradation due to strand bending and inter-filament current transfer", *Cryogenics*, Vol.50, pp.149-157, 2010.

[4] J.W. Ekin, "Effect of stress on the critical current of Nb_3Sn multi-filamentary composite wire," *Appl. Phys. Lett*., vol.29, pp.216-219, 1976.

[5] J.W. Ekin, "Effect of transverse compressive stress on the critical current and upper critical field of Nb_3Sn," *J. Appl. Phys*., vol.62, pp.4829-4834, 1987.

[6] N. Mitchell, "Mechanical and magnetic load effects in Nb_3Sn cable-in-conduit conductors", *Cryogenics*, Vol.43, pp.255-270, 2003.

[7] A. Nijhuis and Y. Ilyin, "Transverse load optimization in Nb_3Sn CICC design: influence of cabling, void fraction and strand stiffness," Supercond. Sci. Technol., vol.19, pp.945-962, 2006.

[8] http://fusionforenergy.europa.eu/mediacorner/newsview.aspx?content=691&utm_source=F4E+News+Subsribers&utm_campaign=992b8a7b21-F4E_News_April_20134_26_2013&utm_medium=email

[9] S. Timoshenko, *Strength of Materials*, Part II: Advanced Theory and Problems, Krieger Publishing Company, Malabar, FL, 1976, pp.54-56.

[10] C. Calzolaio, P. Bruzzone, and D. Uglietti, "Measurement of T_c distribution in Nb_3Sn CICC," *Supercond. Sci. Technol*., 054007, 2012.

[11] Y. Zhai, P. Bruzzone, and C. Calzolaio, "FEMCAM analysis of SULTAN test results for ITER Nb_3Sn cable-in-conduit conductors," submitted for publication.

[12] A. Nijhuis et al, "Axial and transverse stress-strain characterization of the EU dipole high current density Nb_3Sn strand," *Supercond. Sci. Technol.* vol.21, 065011, 2008.

[13] A. Nijhuis et al, "Summary of ITER TF Nb3Sn strand testing under axial strain, spatial periodic bending and contact stress," *IEEE Trans. App. Supercond.* Vol.19, no.3, pp.1516-1520, 2009.

[14] A. Nijhuis et al, "The effect of axial and transverse loading on the transport properties of ITER Nb_3Sn strands," *Supercond. Sci. Technol.* vol.26, 084004, 2013.

The Princeton Plasma Physics Laboratory is operated
by Princeton University under contract
with the U.S. Department of Energy.

Information Services
Princeton Plasma Physics Laboratory
P.O. Box 451
Princeton, NJ 08543

Phone: 609-243-2245
Fax: 609-243-2751
e-mail: pppl_info@pppl.gov
Internet Address: http://www.pppl.gov